Bulletin of Electrochemistry 13 (12) December 1997, pp 441-447

0256-1654/97/$ 3-50

SYNERGISTIC AND BIOCIDAL EFFECTS OF HEDP-Zn^{2+}- CTAB SYSTEM ON THE INHIBITION OF CORROSION OF MILD STEEL IN NEUTRAL AQUEOUS ENVIRONMENT

S RAJENDRAN, B V APPARAO* AND N PALANISWAMY**

G.T.N. Arts College (Autonomous), Dindigul 624 005. INDIA
* Regional Engineering College, Warangal 506 004. INDIA
** Central Electrochemical Research Institute, Karaikudi 630 006. INDIA

[Received: 30 June 1997 Accepted: 17 September 1997]

The synergistic effect of HEDP and Zn^{2+} on the inhibition of corrosion of mild steel in neutral aqueous environment containing 60 ppm chloride has been evaluated by the classical weight-loss method. It is found that the formulation consisting of 50 ppm HEDP and 50 ppm Zn^{2+} offers an inhibition efficiency of 98%. Addition of a biocide viz., N-cetyl-N, N, N-trimethylammonium bromide (CTAB), to the above formulation, upto a concentration of 100 ppm does not reduce the inhibition efficiency. It is interesting to note that the formulation consisting of 50 ppm HEDPP, 50 ppm Zn^{2+} and 50 ppm CTAB has 99% corrosion inhibition effciency and 100% biocidal efficiency. The mechanistic aspects of corrosion inhibition have been studied, in a holistic way, based on the results obtained from polarisation study, X-ray diffraction technique, uv-visible reflectance, FTIR and luminescence spectra. It is observed that the protective film consists of Fe^{2+} -HEDP complex, Fe^{2+} -CTAB complex and $Zn(OH)_2$. The protective film is found to be luminescent.

Keywords: HEDP-Zn^{2+} -CTAB, biocide, corrosion inhibition, synergistic effect, neutral aqueous medium.

INTRODUCTION

Several studies on the use of phosphoric acids as corrosion inhibitors have been reported in the literature [1-11]. Eventhough several papers have discussed the use of 1-hydroxyethane-1, 1-diphosphonic acid (HEDP) as corrosion inhibitor [1-5] the mechanistic aspects of corrosion inhibition has not been studied in detail. In the present study, the synergistic effect of HEDP and Zn^{2+} on the inhibition of corrosion of mild steel in neutral aqueous environment containing 60 ppm Cl^- has been evaluated. The mutual influence this inhibitor system and the biocide, N-cetyl-N,N,N-trimethylammonium bromide (CTAB) has also been studied. The mechanistic aspects are based, in a holistic way, on the results obtained from potentiostatic polarisation study, X-ray diffraction technique, uv-visible, FTIR and luminescence spectra.

EXPERIMENTAL

Preparation of the specimens

Mild steel specimens (0.02 to 0.03% S, 0.03 to 0.08%P, 0.4 to 0.5% Mn, 0.1 to 0.2% C and the rest iron) of the dimensions 1 x 4 x0.2 cm were polished to mirror finish and degreased with trichloroethylene and used for the weight-loss method and surface examination studies. For potentiostatic polarisation studies, mild steel rod encapsulated in Teflon with an exposed cross section of 0.5 cm diameter was used as the working electrode. Its surface was polished to mirror finish and degreased with trichloroethylene.

Weight-loss method

Mild steel specimens, in triplicate, were immersed in 100 ml of the solutions containing various concentrations of the inhibitor in the absence and presence of Zn^{2+}, for a period

of seven days. The weights of the specimens before and after immersion were determined using Mettler balance, AE-240.

Potentiostatic polarisation study

This study was carried out in a three electrode cell assembly connected to Bioanalytical system (BAS - 100 A) electrochemical analyser, provided with iR compensation facility, using mild steel as the working electrode, platinum as the counter electrode and saturated calomel electrode as the reference electrode.

Surface examination study

The mild steel specimens were immersed in various test solutions for a period of two days. After two days, the specimens were taken out and dried. The nature of the film formed on the surface of the metal specimens was anslysed by various surface analysis techniques.

FTIR spectra

The FTIR spectra were recorded using Perkin-Elmer 1600 FTIR spectrophotometer.

UV-visible spectra

The uv-visible reflectance spectra were recorded using Hitachi U- 3400 spectrophotometer.

X-ray diffraction techique

The XRD patterns of the film formed on the metal surface were recorded using a computer controlled X-ray powder diffractometer, JEOL JDX 8030 with CuK_α (Ni-filtered) radiation (λ = 1.5418 A) at a rating of 40 kV, 20 mA. The scan rate was 0.05-20° per step and the measuring time was 1 second per step.

Luminescence spectra

The luminescence spectra of the film formed on the metal surface were recorded using Hitachi 650-10 S fluorescence spectrophotometer equipped with 150 W Xenon lamp and a Hamamatsu R 928 F photomultiplier tube. The emission spectra were corrected for the spectral response of the photomultiplier tube.

Determination of the biocidal efficiency of the system

The biocidal efficiency of the system was determined using Zobell medium and calculating the number of colony forming units per ml, using a bacterial colony counter.

RESULTS AND DISCUSSION

Analysis of the results of the weight-loss method

The corrosion rates of mild steel in neutral aqueous environment containing 60 ppm Cl^- in the absence and presence of inhibitors obtained by the weight-loss method are given in Table I. The corrosion inhibition efficiencies of various systems are also given in Table I. It is observed from Table I that while 50 ppm HEDP alone has only 11% inhibition efficiency, 50 ppm Zn^{2+} is found to be corrosive. Interestingly the formulation consisting of 50 ppm HEDP and 50 ppm Zn^{2+} has 98% inhibition efficiency. This indicates the synergistic effect between HEDP and Zn^{2+}.

Effect of N-cetyl-N,N,N-trimethylammonium bromide (CTAB) on the inhibition efficiency of HEDP-Zn^{2+} system

The corrosion rates of mild steel in neutral aqueous environment containing 60 ppm Cl^-, in the presence and absence of inhibitor and various concentrations of CTAB obtained by weight-loss method are given in Table II. The inhibition efficiencies are also given in Table II.

It is observed from these results that CTAB by itself or in combination with either HEDP or Zn^{2+} does not act as a good inhibitor. It is found that CTAB, upto a concentration of 100 ppm, does not reduce the inhibition efficiency of HEDP-Zn^{2+} system. However, a decrease in corrosion inhibition efficiency of HEDP-Zn^{2+} system is noticed when the CTAB concentration is 150 ppm.

TABLE I: Corrosion rates of mild steel in neutral aqueous environment (Cl^- = 60 ppm) in the presence and absence of inhibitor and the inhibition efficiencies obtained by the weight-loss method
Inhibitor system: HEDP + Zn^{2+}

Concn of HEDP ppm	Concn of Zn^{2+} ppm	Corrosion rate mdd	Inhibition efficiency %
0	0	15.54	—
50	0	13.83	11
50	10	12.12	22
50	50	0.37	98
50	100	0.35	98
50	150	0.31	98
50	200	0.29	98
50	300	0.25	98
0	50	19.11	-23

TABLE II: Corrosion rates of mild steel in neutral aqueous environment (Cl^- = 60 ppm) in the presence and absence of inhibitor and the inhibition efficiencies obtained by the weight-loss method
Inhibitor system: HEDP + Zn^{2+} + CTAB

Concn of HEDP ppm	Concn of Zn^{2+} ppm	Concn of CTAB ppm	Corrosion rate mdd	Inhibition efficiency %
0	0	0	15.54	—
0	0	50	13.99	10
0	50	50	14.76	5
50	0	50	13.83	11
50	50	0	0.37	98
50	50	10	0.16	99
50	50	50	0.16	99
50	50	100	0.16	99
50	50	150	3.00	81
50	50	200	6.22	60

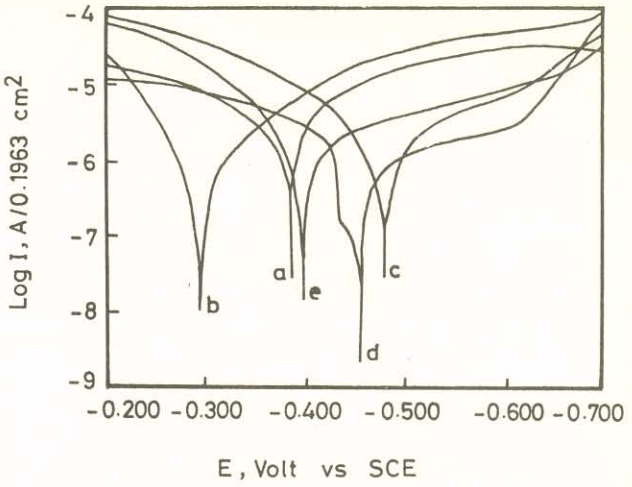

Fig. 1: Potentiostatic polarisation curves of mild steel in various environments
(a) Cl^- 60 ppm (b) Cl^- 60 ppm + CTAB 50 ppm
(c) Cl^- 60 ppm + Zn^{2+} 50 ppm
(d) Cl^- 60 ppm + Zn^{2+} 50 ppm + HEDP 50 ppm
(e) Cl^- 60 ppm + Zn^{2+} 50 ppm+HEDP 50 ppm + CTAB 50 ppm

Effect of HEDP-Zn^{2+} formulation on the biocidal efficiency of CTAB

The biocidal efficiency of CTAB in the presence of HEDP-Zn^{2+} formulation is given in Table III. Though calculations show 99.99 percent biocidal efficiency when the concentration of CTAB is 10 ppm (cf. Table III), the colony forming units/ml are still 1.6 x 10^3, which are objectionable. Therefore, the CTAB concentration of 50 ppm which leaves nil colony forming units is the optimum concentration required. It is seen from these results that when the CTAB concentration is ≥ 50 ppm, no colonies are found in the petri dishes, indicating that these formulations offer 100 percent biocidal efficiency.

TABLE III: Biocidal efficiencies of various environments system: Mild steel immersed in HEDP + Zn^{2+} + CTAB

Concn of Cl^- ppm	Concn of HEDP ppm	Concn ofZn^{2+} ppm	Concn of CTAB ppm	Colony forming unit (ml)	Biocidal efficiency %
60	0	0	0	1 x 10^8	—
60	50	50	0	1 x 10^6 to 1x10^7	90.00
60	50	50	10	1.6 x 10^3	99.99
60	50	50	50	nil	100.00
60	50	50	100	nil	100.00
60	50	50	150	nil	100.00
60	50	50	200	nil	100.00

Thus it is found from Tables II and III that the formulation consisting of 50 ppm HEDP, 50 ppm Zn^{2+} and 50 ppm CTAB offers 100 percent biocidal efficiency and 99 percent corrosion inhibition efficiency.

Analysis of the results of potentiostatic polarisation study for the HEDP-Zn^{2+}-CTAB system

The potentiostatic polarisation curves of mild steel immersed in the environments in the presence and absence of CTAB are given in Fig. 1. It is evident from Fig. 1 that when 50 ppm CTAB is added to the solution containing 60 ppm Cl^- the corrosion potential shifts from -389 mV vs SCE to -293 mV vs SCE (anodic shift). The formulation consisting of 50 ppm HEDP+50 ppm Zn^{2+} shifts the corrosion potential -400 mV vs SCE. These results suggest that the formulation

TABLE IV: Corrosion parameters of mild steel in neutral aqueous environment (Cl^- = 60 ppm) in the presence and absence of inhibitor obtained by polarisation method
Inhibitor system: HEDP + Zn^{2+} + CTAB

Concn of HEDP ppm	Concn of Zn^{2+} ppm	Concn of CTAB ppm	E_{corr} mV vs SCE	b_c mV	b_a mV
0	0	0	-389	95	120
0	50	0	-489	125	115
0	0	50	-293	93	132
50	50	0	-470	125	150
50	50	50	-400	122	152

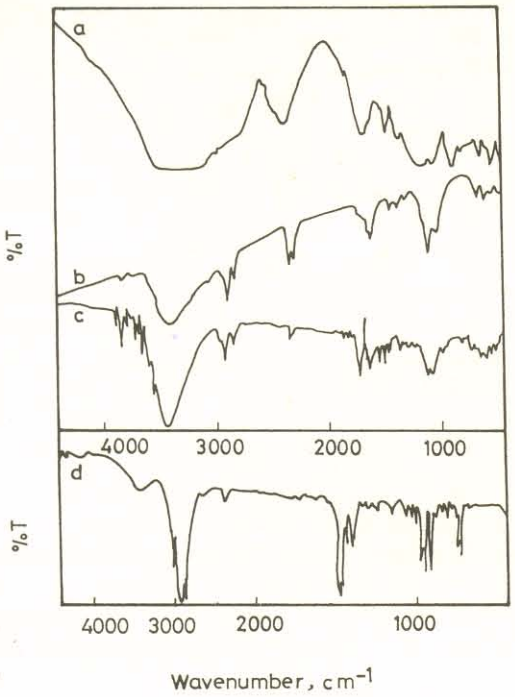

Fig. 2: FTIR spectra of HEDP (a), CTAB (b) and of mild steel surface immersed in various environments (b,c)
(a) Pure HEDP
(b) Cl^- 60 ppm + HEDP 50 ppm + Zn^{2+} 50 ppm
(c) Cl^- 60 ppm+HEDP 50 ppm+Zn^{2+} 50 ppm + CTAB 50 ppm
(d) Pure CTAB

consisting of HEDP, Zn^{2+} and CTAB functions as a mixed inhibitor.

These views are further supported by the shifts in anodic and cathodic Tafel slopes (Table IV). It is observed that addition of 50 ppm CTAB to the system consisting of ppm Cl^- shifts the anodic slope to a large extent (12 mV/decade) and the cathodic slope to a small extent (2 mV/decade). When CTAB is added to HEDP-Zn^{2+} combination, both the anodic and cathodic slopes are shifted almost equally (32 mV/decade and 27 mV/decade, respectively). That means the shift in anodic slope is only slightly greater than the shift in cathodic slope. It is inferred from these results that while CTAB alone controls predominantly the anodic process, the HEDP-Zn^{2+}-CTAB combination controls both the anodic process and cathodic process; the anodic process to a slightly larger extent. Thus, HEDP-Zn^{2+}-CTAB formulation also functions as a mixed inhibitor.

Analysis of the FTIR spectra

The FTIR spectra of pure HEDP and CTAB are given in Figs. 2a and d.

The FTIR spectrum of the film scratched from the surface of the metal immersed in the environment consisting of 60 ppm Cl^-, 50 ppm HEDP and 50 ppm Zn^{2+} is given in Fig. 2b. It is observed that the P-O stretching frequency has decreased from 1119 cm^{-1} to 1047.6 cm^{-1}. This shift is caused by the decrease of electron cloud density of the P-O bond. Due to the shift of the electron cloud density from the oxygen atom to Fe^{2+}, it is suggested that the oxygen atom of the phosphonic acid is coordinated to Fe^{2+} resulting in the formation of Fe^{2+}-HEDP complex on the metal surface [12-16]. The band at 1357.1 cm^{-1} is due to $Zn(OH)_2$ [1,5,8,9,11,17].

The FTIR spectrum of the film scratched from the surface of the metal immersed in the solution containing 60 ppm Cl^-, 50 ppm HEDP, 50 ppm Zn^{2+} and 50 ppm CTAB is given in Fig. 2c. It is seen from the spectrum that the P-O stretching frequency of HEDP has shifted from 1119 cm^{-1} to 1071.4 cm^{-1}. This indicates that formation of Fe^{2+}-HEDP complex on the metal surface [12-16]. The band due to $Zn(OH)_2$ appears at 1373.2 cm^{-1} [1,5,8,9,11,17]. It is also inferred that the band at 1122.1 cm^{-1} corresponds to C-N stretching. The band at 2857.1 cm^{-1} is due to ν_s CH_3. The absorption band due to ν_{as} CH_2 appears at 2928.6 cm^{-1}. The band at 2857.1 cm^{-1} represents ν_s CH_2 [12]. These bands clearly indicate the presence of CTAB on the metal surface, probably as Fe^{2+}-CTAB complex.

Analysis of the UV-visible reflectance spectra

The uv-visible reflectance spectra of the surfaces of the metal specimens immersed in various environments are given in

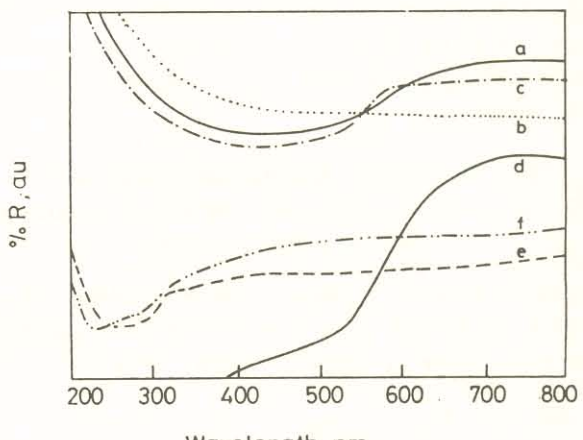

Fig. 3: UV-visible reflectance spectra of mild steel surface immersed in various environments
(a) Unpolished metal (b) Polished metal
(c) Polished metal + Cl^- 60 ppm
(d) Cl^- 60 ppm + Zn^{2+} 50 ppm
(e) Cl^- 60 ppm + Zn^{2+} 50 ppm + HEDP 50 ppm
(f) Cl^- 60 ppm+Zn^{2+} 50 ppm + HEDP 50 ppm + CTAB 50 ppm

Fig. 3. The uv-visible reflectance spectrum of the unpolished metal, of the polished metal immersed in the environment containing 60 ppm Cl^-, and that of the polished metal immersed in the environment consisting of 60 ppm Cl^- and 50 ppm Zn^{2+}, show wavelength transition at 550 nm revealing that the band gap (E_g) of the film formed on the above surfaces is E_g = 1.239/0.55 = 2.25 eV. This indicates that the films formed on the above surfaces consist of oxides of iron [18- 20] having semiconducting property [21-24].

On the other hand, the uv-visible reflectance spectrum of the polished metal does not show any wavelength transition at 550 nm.

The uv-visible reflectance spectrum of the film formed on the surface of the metal specimen immersed in the environment consisting of 60 ppm Cl^- + 50 ppm HEDP+50 ppm Zn^{2+} reveals the absence of wavelength transition at 550 nm, thus resembling that of a polished metal.

It is seen from the uv-visible reflectance spectrum of the surface of the metal immersed in the environment consisting of 60 ppm Cl^-, 50 ppm HEDP, 50 ppm Zn^{2+} and 50 ppm CTAB, that the metal surface in this environment, in the presence of CTAB also resembles the polished metal surface, without wavelength transition at 550 nm. It is speculated that the absorptions at 230 nm and 260 nm are due to the Fe^{2+}-CTAB and Fe^{2+}-HEDP complexes on the metal surface, respectively.

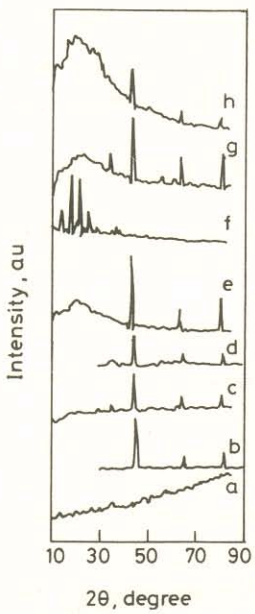

Fig. 4: XRD patterns of pure CTAB (f) and of mild steel surface immersed in various environments
(a) Unpolished metal (b) Polished metal
(c) Polished metal + Cl^- 60 ppm
(d) Cl^- 60 ppm + Zn^{2+} 50 ppm
(e) Cl^- 60 ppm + Zn^{2+} 50 ppm + HEDP 50 ppm
(f) Pure CTAB (g) Cl^- 60 ppm + CTAB 50 ppm
(h) Cl^- 60 ppm+Zn^{2+} 50 ppm + HEDP 50 ppm + CTAB 50 ppm

Analysis of the X-ray diffraction patterns

The x-ray diffraction (XRD) patterns of the films formed on the surfaces of the metal specimens immersed in various test solutions are given in Fig. 4.

The surface of the unpolished metal contains t-FeOH (2θ = 13.6°), Fe_3O_4 (2θ = 35.7°) and α-FeOOH (2θ = 58.2°). The peak due to iron occurs at 2θ = 44.2° [25]. In the case of polished metal, the peaks due to iron appear at 2θ = 44.8°, 65.1° and 82.4°. With the metal specimen immersed iin 60 ppm Cl^- solution, in addition to iron peaks, peaks due to magnetite (Fe_3O_4) occur at 2θ = 30.1°, 35.5° and 62.5° [25]. This indicates that in the chloride environment, mild steel specimen has undergone corrosion, leading to the formation of magnetite.

The film formed on the surface of the metal immersed in the environment consisting of 60 ppm Cl^- and 50 ppm Zn^{2+} consists of Fe_3O_4 (2θ = 35.4°). The peaks due to iron appear at 2θ = 44.8°, 65.1° and 82.5° [25].

The XRD pattern of the surface of the metal specimen immersed in the environment consisting of 60 ppm Cl^-, 50 ppm HEDP and 50 ppm Zn^{2+} indicates the absence of any kind of oxides of iron such as α- FeOOH, t-FeOOH and Fe_3O_4 [25].

The XRD pattern of pure CTAB is given in Fig. 4f. The peak with relative intensity of 100 percent apppears at 2θ = 18.9°.

The XRD pattern of the surface of the metal immersed in the environment containing 60 ppm Cl^- and 50 ppm CTAB is given in Fig. 4g. It is observed that Fe_3O_4 (2θ = 35.4°, 37.1°, 43.2°, 57.2° and 62.6°) and α-FeOOH (2θ = 39.99°) are present on the metal surface [25].

The XRD pattern of the surface of the metal immersed in the environment consisting of 60 ppm Cl^-, 50 ppm HEDP, 50 ppm Zn^{2+} and 50 ppm CTAB (Fig. 4h) shows the presence of iron peaks only (2θ = 44.7°, 65.0° and 82.1°) and absence of any oxides of iron [25]. The presence of CTAB on the surface of the metal is revealed by the peak at 2θ = 8.9°, since this peak occurs in the XRD patterns of pure CTAB also and has 100 percent relative intensity (in the latter pattern).

Analysis of the luminescence spectra

The luminescence spectra (λ_{ex} = 270 nm) of the surface of the metal immersed in various environments are given in Figs. 5a to c. It is observed that the intensities of the peaks are increased by the addition of 50 ppm Zn^{2+} to the system consisting of 60 ppm Cl^- and 50 ppm HEDP (Figs. 5a and b). This suggests that the formation of Fe^{2+}- HEDP complex is enhanced in the presence of Zn^{2+}. Addition of 50 ppm CTAB to the above system changes the pattern of the spectrum in the region of 290 nm to 410 nm (Fig. 5c). This may be due to the formation of Fe^{2+}-HEDP complex and also Fe^{2+}-CTAB complex on the metal surface.

Mechanism of corrosion inhibition

Anlysis of the results of the weight-loss method and biocidal efficiency estimation reveals that the formulation consisting of 50 ppm HEDP, 50 ppm Zn^{2+} and 50 ppm CTAB offers 99 percent corrosion inhibition efficiency and 100 percent biocidal efficiency. Results of polarisation study show that this formulation acts as a mixed inhibitor. FTIR spectra show the presence of Fe^{2+}-HEDP complex, Fe^{2+}-CTAB complex and $Zn(OH)_2$ on the inhibited metal surface. The uv-visible reflectance spectra and XRD pattern show that the metal surface, in the presence of the protective film, resembles the polished metal surface. The protective film is found to be luminescent. In order to explain all these observations in holistic way, the following mechanism of corrosion inhibition is proposed:

1. When the environment containing 60 ppm Cl^-, 50 ppm HEDP, 50 ppm Zn^{2+} and 50 ppm CTAB is prepared, there is formation of both the Zn^{2+}-HEDP complex and Zn^{2+}-CTAB complex in solution.
2. When the metal is immersed in this environment, the Zn^{2+}-HEDP complex and Zn^{2+}-CTAB complex diffuse from the bulk of the solution to the surface of the metal.
3. On the surface of the metal, Zn^{2+}-HEDP complex is converted into Fe^{2+}-HEDP complex in the local anodic sites, since the latter is more stable than the former.

$$Zn^{2+}\text{-HEDP} + Fe^{2+} \rightarrow Fe^{2+} - \text{HEDP} + Zn^{2+}$$

4. Similarly Zn^{2+}-CTAB complex is converted into Zn^{2+}-CTAB complex iin the local anodic sites:

$$Zn^{2+}\text{-CTAB} + Fe^{2+} \rightarrow -XTAB + Zn^{2+}$$

(Formation of Fe^{3+}-HEDP complex and also Fe^{3+}-CTAB complex to some extent cannot be ruled out.)

5. The released Zn^{2+} ions on the metal surface form $Zn(OH)_2$ in the local cathodic regions.

$$Zn^{2+} + 2OH^- \rightarrow Zn(OH)_2$$

6. Thus, the protective film consists of Fe^{2+}-HEDP complex, Fe^{2+}-CTAB complex and $Zn(OH)_2$.

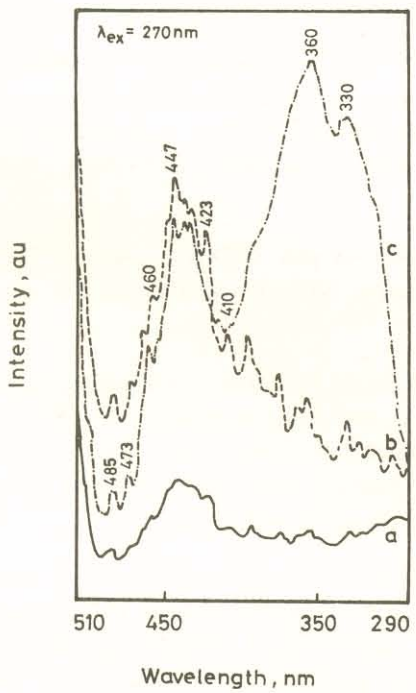

Fig. 5: Luminescence spectra of mild steel surface immersed in various environments (a) Cl^- 60 ppm + HEDP 50 ppm (b) Cl^- 60 ppm + Zn^{2+} 50 ppm + HEDP 50 ppm (c) Cl^- 60 ppm+Zn^{2+} 50 ppm + HEDP 50 ppm + CTAB 50 ppm

CONCLUSION

1. The formulation consisting of 50 ppm HEDP, 50 ppm Zn^{2+} and 50 ppm CTAB offers 99% corrosion inhibition efficiency and 100% biocidal efficiency to mild steel immersed in the neutral aqueous environment containing 60 ppm Cl^-.
2. The protective film consists of Fe^{2+}-HEDP complex, Fe^{2+}-CTAB complex and $Zn(OH)_2$.
3. The protective film is found to be luminescent.
4. The above formulation can be used in cooling water systems.

Acknowledgement: S.Rajendran is thankful to the University Grants Commission, New Delhi, India, for financial assistance, to Mr. Ranjit Soundarajan, the Correspondent, Prof. S.Ramakrishnan, the Principal, and Prof. P.Jayaram, Head of the Chemistry Department,

G.T.N.Arts College, Dindigul and to Prof. G.Karthikeyan, Head of the Chemistry Department, Gandhigram University, for their encouragement.

REFERENCES

1. I Sekine and Y Kirakawa, *Corrosion,* **42** (1986) 272
2. A Veres, G Reinhard and E Kalman, *Brit Corrosion J,* **27** (1992) 147
3. E Kalman, B Varhegyi, I Bako, I Felhosi, F H Karman and A Shaban, *J Electrochem Soc,* **141** (1994) 3357
4. T Galkin, V A Kotenev, M Arponen, O Forsen and S Ylasaari, *Proc 8th Europ Symp Corrosion Inhibitors,* Ferrara, Italy, **1** (1995) 25
5. S Rajendran, B V Apparao and N Palaniswamy, *EUROCORR'96 Nice,* Paper No.II-P 1
6. S T Hirozawa, *Proc 8th Europ Symp Corrosion Inhibitors,* Ferrara, Italy, **1** (1995) 25
7. T Galkin, O Forsen, S Ylasaari, V A Kotenev and M Arponen, *EUROCORR'96 Nice,* Paper No.II-OR 2
8. S Rajendran, B V Apparao and N Palaniswamy, *Bull Electrochem,* **12** (1996) 15
9. S Rajendran, B V Apparao and N Palaniswamy, *Proc Second Arabian Corrosion Conference,* Kuwait Institute for Scientific Research, Kuwait, (1996) 483
10. J L Fang, Y Li, X R Ye, Z W Wang and Q Liu, *Corrosion,* **49** (1993) 266
11. S Rajendran, B V Apparao and N Palaniswamy, *Proc 8th Europ Symp Corrosion Inhibitors,* Ferrara, Italy, **1** (1995) 465
12. R M Silverstein, G C Bassler and T C Morrill, *"Spectrometric Identification of Inhibitors,* Ferrara, Italy, **1** (1995) 465
13. K Nakamoto, *"Infrared and Raman Spectra of Inorganic and Coordination Compounds",* Wiley-Interscience, New York, (1986) 168
14. A D Cross, *"Introduction to Practical Infra-red Spectroscopy",* Butterworths Scientific Publication, London (1960) 73
15. T D J Smith, *Inorg Nucl Chem,* **9** (1959) 150
16. L Horner and C L Horner, *Werkst Korros,* **27** (1976) 223
17. E D Mor and C Wrubl, *Brit Corrosion J,* **11** (1976) 199
18. M Sharon, G Tamizhamani and K Basaraswaram, *Proc Indian Nat Sci Acd,* **52** (1986) 311
19. H L Sanchez, H Steinfink and H S White, *J Solid State Chem,* **41** (1982) 90
20. C Sanchez, K D Sieber and G A Somorjai, *J Electroanal Chem,* **252** (1988) 269
21. W Schultze and U Stimming, *Z Phys Chem,* N.F., **98** (1975) 285
22. S M Wilhelm, K S Yun, L W Ballenger and N Hackerman, *J Electrochem Soc,* **126** (1979) 416
23. S M Wilhelm and N Hackerman, *J Electrochem Soc,* **128** (1981) 1668
24. L M Abrantes and L M Peter, *J Electroanal Chem, **150** (1983) 593*
25. M Favre and D Landolt, *Corrosion Science,* **34** (1993) 1481